Journal of Pathology
J Pathol 2012; **226:** 598–608
Published online 5 December 2011 in Wiley Online Library (wileyonlinelibrary.com) DOI: 10.1002/path.3009

ORIGINAL PAPER

Severity of doxorubicin-induced small intestinal mucositis is regulated by the TLR-2 and TLR-9 pathways

Agnieszka Kaczmarek,[1,2] Brigitta M Brinkman,[1,2] Liesbeth Heyndrickx,[1,2] Peter Vandenabeele[1,2]*† and Dmitri V Krysko[1,2]*†

[1] *Department for Molecular Biomedical Research, VIB, Ghent, Belgium*
[2] *Department of Biomedical Molecular Biology, Ghent University, Ghent, Belgium*

**Correspondence to: Peter Vandenabeele, Department for Molecular Biomedical Research, VIB-Ghent University, Technologiepark 927, B-9052 Ghent (Zwijnaarde), Belgium. e-mail: Peter.Vandenabeele@dmbr.UGent.be*
**Correspondence to: Dmitri V Krysko, Department for Molecular Biomedical Research, VIB-Ghent University, Technologiepark 927, B-9052 Ghent (Zwijnaarde), Belgium. e-mail: Dmitri.Krysko@dmbr.UGent.be*

†These authors contributed equally to this work.

Abstract

Intestinal mucositis is a serious complication of cancer chemotherapy and radiotherapy; it frequently compromises treatment and dramatically reduces the quality of life of patients. Different approaches to limit the damage to the intestine during anti-cancer therapy have been largely ineffective due to insufficient knowledge of the mechanism of mucositis development. This study aimed to define the role of TLR-2 and TLR-9 in the modulation of small intestinal damage in a model of doxorubicin-induced mucositis. Doxorubicin-induced intestinal damage was verified by a histological score (HS), analysis of leukocyte influx into the lamina propria, and determination of the number of apoptotic cells. Additionally, the activation status of glycogen synthase kinase 3β (GSK-3β) was assessed. Wild-type (WT) mice injected with doxorubicin demonstrated severe intestinal damage (HS 8.0 ± 0.81), reduction of villus length to 43.9% ± 13.7% of original length, and increased influx of leukocytes as compared to vehicle-injected mice (HS 1.33 ± 1.15). The protective effect of TLR-2 or TLR-9 deficiency was associated with a significant decrease of the HS as compared to WT mice. In the ileum, a minor reduction of villus length and a decreased number of infiltrating leukocytes and TUNEL-positive cells was observed. We demonstrate that the TLR-9 antagonist ODN2088 reduces doxorubicin-induced intestinal damage. Furthermore, we show that GSK-3β activity is inhibited in the absence of TLR-2. The protective capacity of GSK-3β suppression was observed in WT mice by inhibiting it with the specific inhibitor SB216763. Overall, our findings demonstrate that the TLR-2/GSK-3β and TLR-9 signalling pathways play a central role in the development of intestinal mucositis and we suggest a new therapeutic strategy for limiting doxorubicin-induced intestinal inflammation.

Keywords: chemotherapy-induced mucositis; small intestine damage; apoptosis; ileitis; inflammation

Received 8 April 2011; Revised 13 September 2011; Accepted 23 September 2011

No conflicts of interest were declared.

Introduction

Mucosal barrier injury (MBI, mucositis) of the gastrointestinal tract (GIT) remains a serious side effect of cancer chemotherapy and radiotherapy. Oral mucositis is painful and the most frequent complication [1]. Gut MBI, however, is a real danger because it goes unrecognized, yet predisposes patients to serious clinical complications, including increased risk of infections and bleeding leading to prolonged hospitalization. It also dictates dose reduction in the subsequent chemotherapy cycle, which slows or hinders cure of the disease [2,3].

The mechanism of mucositis development is still not fully understood. However, a five-step model formulated by Sonis [4,5] describes an initiation phase of cell injury and NF-κB activation, followed by induction of pro-inflammatory cytokines, which then cause tissue inflammation [6,7] and further cell apoptosis. Massive apoptosis disrupts the epithelial barrier, allowing bacterial translocation from the lumen to the lamina propria, which causes ulceration. Indeed, alterations in intestinal permeability and damage of epithelial continuity have been reported in patients [8,9]. In the final stage, epithelium is renewed and mucositis is resolved.

Intestinal bacteria are recognized by pattern recognition receptors (PRRs), of which Toll-like receptors (TLRs) are the best characterized. TLRs are expressed on intestinal epithelial cells (enterocytes [10], Paneth cells [11], goblet cells [12], and endocrine cells [13]) and professional immune cells of lamina propria [14]. The importance of TLR signalling in intestinal homeostasis and in diseases is now well

established. Recognition of microbes via their microbe-associated molecular patterns (MAMPs) and consequent distinction between commensal bacteria and other microbes have been shown to maintain intestinal homeostasis [15]. Detection of pathogens triggers immune responses involving secretion of antimicrobial peptides [16] and cytokines [17]. Despite the beneficial role of PRRs, deregulation of TLR signalling is also associated with the pathogenesis of inflammatory bowel disease (IBD) and gastrointestinal cancer [18]. Moreover, TLRs were recently recognized as upstream receptors of glycogen synthase kinase 3β (GSK-3β) [19]. GSK-3 regulates multiple transcription factors important in inflammation and cytokine production [20], as well as cell cycle progression and apoptosis [21], and contributes to the pathogenesis of several diseases, including chronic colitis [22].

It has been shown that TLRs could modulate cell death in several model systems [23–25] and that apoptosis precedes intestinal hypoplasia in patients [26]; we therefore hypothesize that TLRs might play a role in the initiation phase of MBI development, not only in the later stages as proposed by Sonis [4]. To address this question, we employed a doxorubicin-induced murine mucositis model to investigate whether TLRs are required for the development of mucositis. We report the novel finding that absence of TLR-2 or TLR-9 results in protection of the small intestine against doxorubicin, most likely by reduction of epithelial cell apoptosis. We also demonstrate that the severity of doxorubicin-induced intestinal mucositis can be reduced by using a TLR-9 antagonist. In addition, we show that the pro-survival effect of TLR-2 deficiency in this model is correlated with inhibition of GSK-3β activity.

Materials and methods

Mice

For the kinetics experiments, female C57BL/6 mice (7–10 weeks old) were purchased from Janvier (Bio Services BV, The Netherlands). We used TLR-2$^{-/-}$ and TLR-9$^{-/-}$ single knockout mice on a C57BL/6 background. Wild-type (WT) C57BL/6 mice were used as controls. WT and TLR-2$^{-/-}$ mice were bred in the FSVM SPF facility. TLR-9$^{-/-}$ and WT mice were bred at the animal facility of the Vrije Universiteit Brussel. All experimental procedures were approved by the local Ethics Committee of Ghent University–VIB.

Doxorubicin-induced intestinal mucositis

Doxorubicin hydrochloride (Sigma-Aldricht, Bornem, Belgium) was freshly dissolved in sterile LPS-free 0.9% NaCl (Braun-NVSA, Diegem, Belgium). Mice were injected intraperitoneally (i.p.) with 10 mg/kg of doxorubicin in 0.2 ml of 0.9% NaCl. Equal volumes of 0.9% NaCl were injected as controls. After mice were euthanized, jejunum and ileum were collected for immunohistochemical evaluation. Mid-jejunum was collected for protein isolation.

Histological evaluation of mucositis

Samples of proximal and distal ileum were fixed in formalin, embedded in paraffin, sectioned at 5 µm, and stained with H&E. Sections were viewed with a light microscope (Axioskop 2, Zeiss). At least 15 random villi per mouse were blind-scored by two independent investigators. For evaluation, we used a modified [27] histological scoring system (HS, ranges from 1 to 12 points; Supporting information, Supplementary Table 1). Villus height and thickness were measured using ImageJ software on images captured with a microscope camera at 20× magnification. Briefly, the height of the intact villus was measured from the base of the villus (opening of the crypt) to the top. Thickness was measured at the base of the villus. At least 15 villi were analysed. The raw measurements in pixels were converted to µm taking into account microscope magnification.

Immunohistochemistry

A standard protocol was used for immunohistochemical (IHC) staining. The primary antibodies were rat anti-mouse F4/80 antigen (1 : 100; MCA497GA, Abd Serotec, Düsseldorf, Germany), CD45 (1 : 250; BD Benelux NV, Temse, Belgium), and biotinylated goat anti-rabbit secondary antibody (DAKO, Heverlee, Belgium). TUNEL assay was performed with the ApopTag® Peroxidase *In Situ* Apoptosis Detection Kit (S7100; Millipore, Billerica, USA) according to the manufacturer's instructions. Sections were counterstained with haematoxylin. Images were taken under a bright field microscope. In the case of CD45 staining, positive cells were counted using ImageJ software and the count was expressed as the percentage of positively stained cells in the viewing field. At least five random fields were examined for each mouse. For TUNEL staining, positively stained cells were counted within crypts and counts were expressed as the average number of apoptotic cells per crypt.

Inhibition of TLR-9 *in vivo*

WT mice were divided into three groups and injected as follows: (1) 50 µg of TLR-9 antagonist ODN2088 (Invivogen, Toulouse, France) together with doxorubicin (10 mg/kg), and 6 h later with another dose of 50 µg of ODN; (2) doxorubicin alone and 6 h later an equal volume of 0.9% NaCl; (3) 0.9% NaCl [28]. Samples were harvested 72 h later and processed as described above.

Inhibition of GSK-3β *in vivo*

GSK-3 activity was blocked with SB216763 (Bio-Connect BV, Huissen, The Netherlands), a known inhibitor of GSK-3α and -β [29]. WT mice were

injected i.p. with 0.6 mg/kg of inhibitor for two consecutive days before doxorubicin administration (10 mg/kg) [30]. The control group received 0.9% NaCl with an equivalent volume of DMSO, which was used to dilute SB216763. Samples were harvested 24 and 72 h later and processed as described above.

Immunoblot analysis

Mid-jejunum segments of about 5 mm were homogenized in 500 µl of caspase lysis buffer [31]. Fifty micrograms of protein was separated by SDS-PAGE and blotted on PVDF membranes. Blots were incubated overnight at 4 °C with Phospho(Ser9)-GSK-3β (1 : 2000; Cell Signaling, Leiden, The Netherlands), washed, and incubated with ECL™ anti-rabbit IgG, HRP-linked whole antibody (1 : 3000; GE Healthcare, Hoevelaken, The Nederlands). Actin staining was used as a loading control. ImageJ software was used to quantify band intensity. Relative density was expressed as the ratio of GSK-3β to actin.

Statistical analysis

All data are given as mean ± SEM. The Mann–Whitney test or one-way ANOVA with the Kruskal–Wallis post-test was used to evaluate the differences between the groups (GraphPad Prism-5 software).

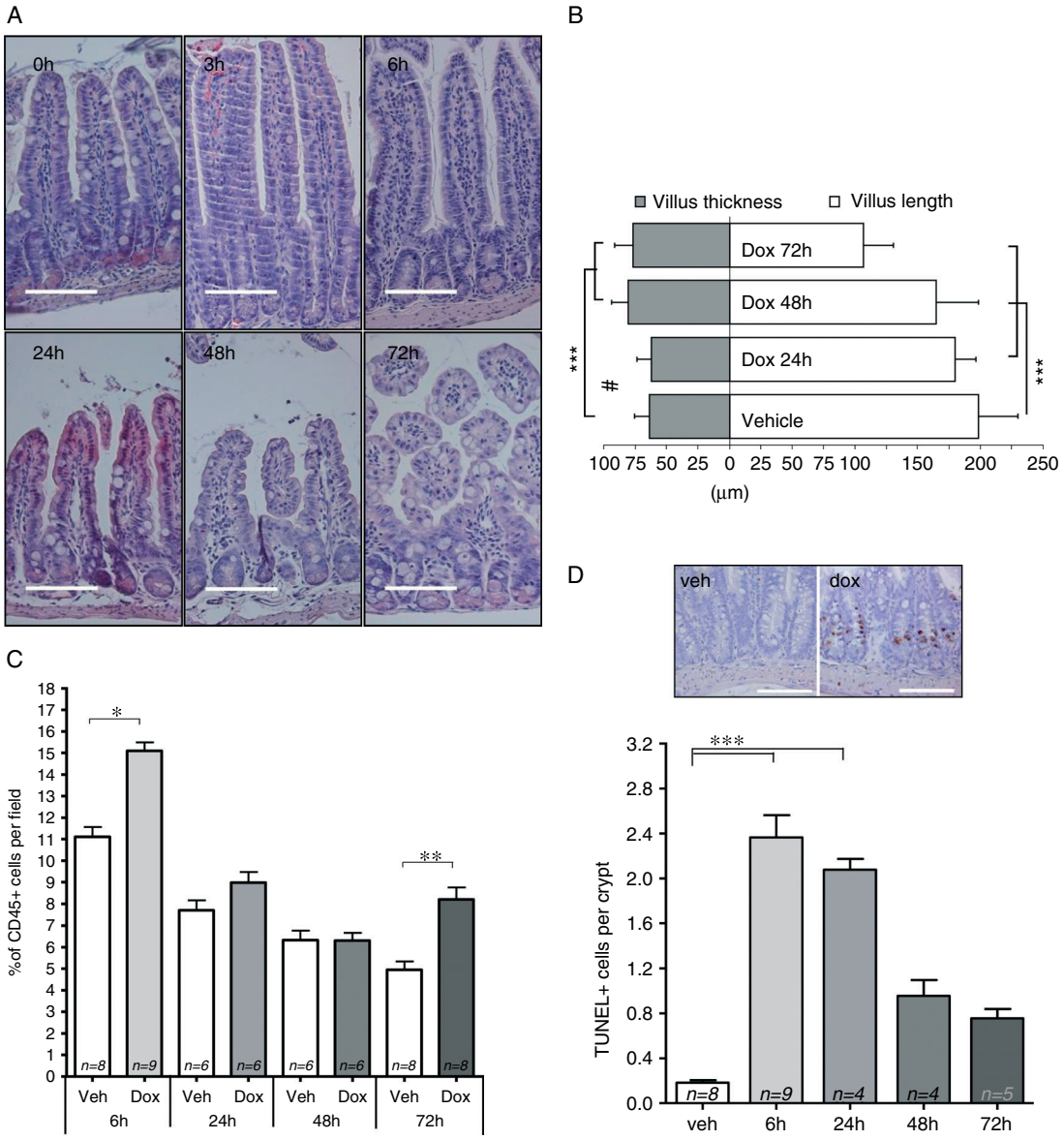

Figure 1. Single intraperitoneal injection of doxorubicin (10 mg/kg) induces time-dependent damage of the small intestine in WT mice. (A) Representative images of H&E-stained sections of the ileum of WT mice 3, 6, 24, 48, and 72 h after doxorubicin injection. Scale bars = 100 µm. (B) Time-dependent changes in villus length (white bars) and thickness (grey bars) after doxorubicin treatment. (C) Significant increase in $CD45^+$ lymphocytes was observed 6 and 72 h after doxorubicin administration. (D) Apoptotic cells were visualized by TUNEL staining and counted 3, 6, 24, 48, and 72 h after doxorubicin injection; counts are expressed as the number of apoptotic cells per crypt. The number of apoptotic cells was elevated 6 h after doxorubicin administration and it remained high 24 h after treatment. Inset: representative images of TUNEL-stained sections 6 h after vehicle or doxorubicin injection. Scale bars = 100 µm. $^{***}p < 0.001$; $^{**}p < 0.01$; $^{*}p < 0.05$; # non-significant difference. $n = 4–9$ mice per group.

$p < 0.05$ was considered statistically significant. n indicates the number of mice per group.

Results

Doxorubicin induces time-dependent damage of the small intestine in wild-type mice

Intestinal morphology was examined to evaluate the influence of doxorubicin on mucositis development. Tissue sections revealed time-dependent changes in ileum structure in response to treatment. Intestinal morphology was normal 3 h post-injection, but the influx of immune cells in the lamina propria was elevated 6 h later. Within 48 h of injection, villus blunting and an amorphic crypt shape were noticeable. Villus and crypt degeneration was most pronounced 72 h after doxorubicin injection relative to other time points (Figure 1A). Quantitative analysis showed time-dependent gradual shortening of villi, leading to their atrophy (Figure 1B).

Having noticed cell infiltration in H&E-stained sections, we examined whether doxorubicin treatment influences immune cell migration from blood vessels to the lamina propria of the intestine. We counted $CD45^+$ leukocytes and $F4/80^+$ macrophages in the ileum. The first large influx of $CD45^+$ leukocytes occurred 6 h after doxorubicin administration and the second was 72 h post-injection (Figure 1C). The number of mature macrophages remained unchanged during the treatment, yet on average it was 1.7 times higher than in the control group (data not shown).

Light microscopic evaluation of TUNEL-stained sections showed a 13-fold increase in apoptotic cell

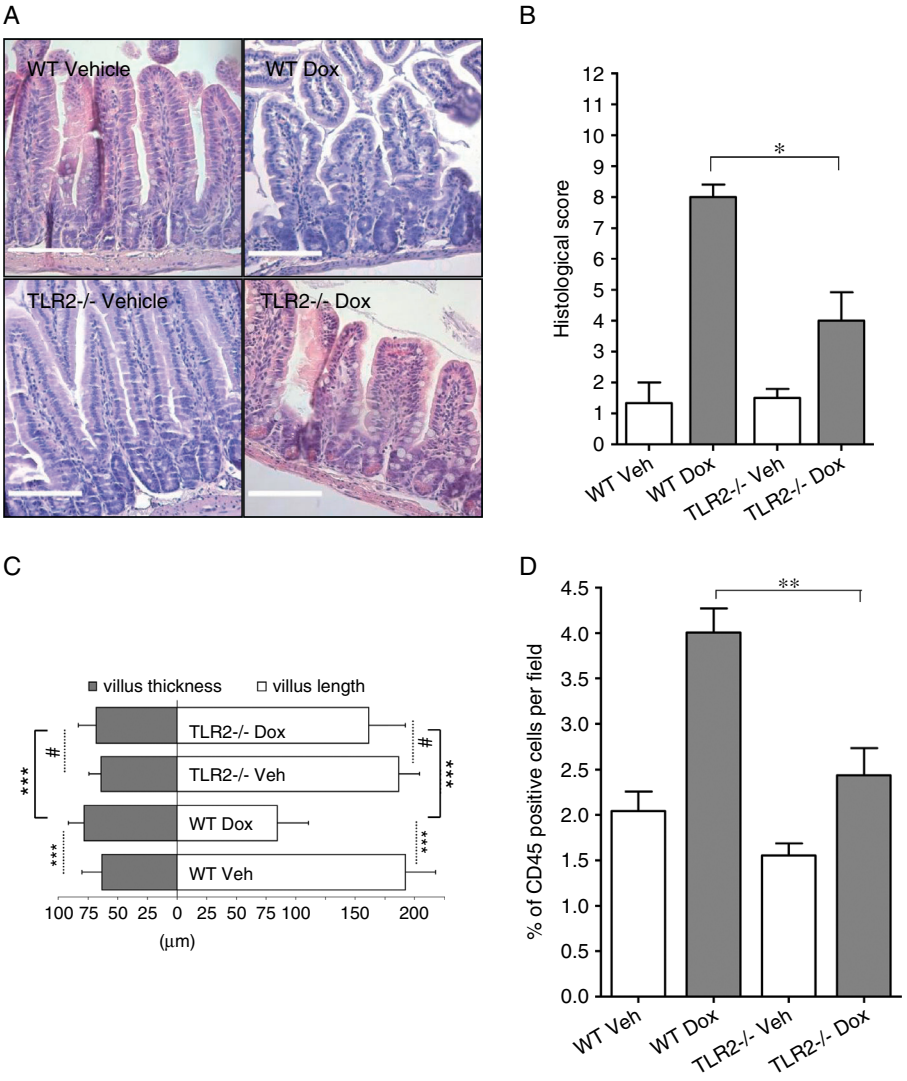

Figure 2. TLR-$2^{-/-}$ mice show milder signs of doxorubicin-induced intestinal mucositis. (A) Representative images of H&E-stained sections of the ileum of WT mice and TLR-$2^{-/-}$ mice 72 h after injection of doxorubicin or vehicle. Histological changes after doxorubicin treatment were less prominent in TLR-$2^{-/-}$ mice than in WT mice. Scale bars = 100 μm. (B) HS in TLR-$2^{-/-}$ mice is lower than in WT mice 72 h after doxorubicin administration. (C) Changes in villus length (white bars) and thickness (grey bars). Villi of TLR-$2^{-/-}$ mice after drug treatment were similar in length and thickness to villi of control mice. (D) Ileum was collected 72 h after doxorubicin or vehicle treatment and sections were stained with the leukocyte marker CD45. Doxorubicin induced influx of leukocytes in WT mice, but the percentage of $CD45^+$ cells in TLR-$2^{-/-}$ mice was significantly lower. $n = 4$ mice per group. $^{***}p < 0.001$; $^{**}p < 0.01$; $^{*}p < 0.05$; # non-significant difference.

number 6 h after doxorubicin treatment (2.36 ± 1.3 cells per crypt) compared with the control group (0.18 ± 0.18). The number of apoptotic cells reached 2.08 ± 0.65 cells per crypt 24 h after doxorubicin treatment, decreased to 0.95 ± 0.24 48 h later, and diminished further to 0.64 ± 0.1 cells 72 h after doxorubicin injection (Figure 1D). Most TUNEL-positive cells were located between cell positions 3 and 6 of the intestinal crypt (Figure 1D).

Absence of TLR-2 or TLR-9 signalling protects from doxorubicin-induced intestinal mucositis

We previously showed that TLR-2 and TLR-9 knockout mice have reduced signs of doxorubicin-induced acute peritonitis [32], but we did not investigate intestinal damage in these mice. To investigate the role of TLR-2 and TLR-9 in doxorubicin-induced intestinal mucositis, we determined the histological scores (HS) [27] of ileal tissue 72 h post-injection.

Doxorubicin induced severe intestinal damage in WT mice (HS 8.0 ± 0.81 compared with 1.33 ± 1.15 in vehicle-injected mice). The ileum of TLR-$2^{-/-}$ mice (HS 4.0 ± 1.82) was significantly less affected than in WT mice, indicating protection against doxorubicin treatment (Figures 2A and 2B). The marked shrinkage and thickening of villi and stroma retraction from enterocytes observed in WT mice were not present in TLR-2-deficient mice (Figures 2A and 2C). $CD45^{+}$ leukocytes in the lamina propria were significantly fewer in $TLR2^{-/-}$ mice than in WT mice (Figure 2D).

Degeneration of the intestine after doxorubicin treatment was also less severe in TLR-$9^{-/-}$ mice (HS 4.25 ± 1.25 compared with 7.75 ± 1.70 in WT mice) (Figures 3A and 3B). Villi of TLR-$9^{-/-}$ mice did not

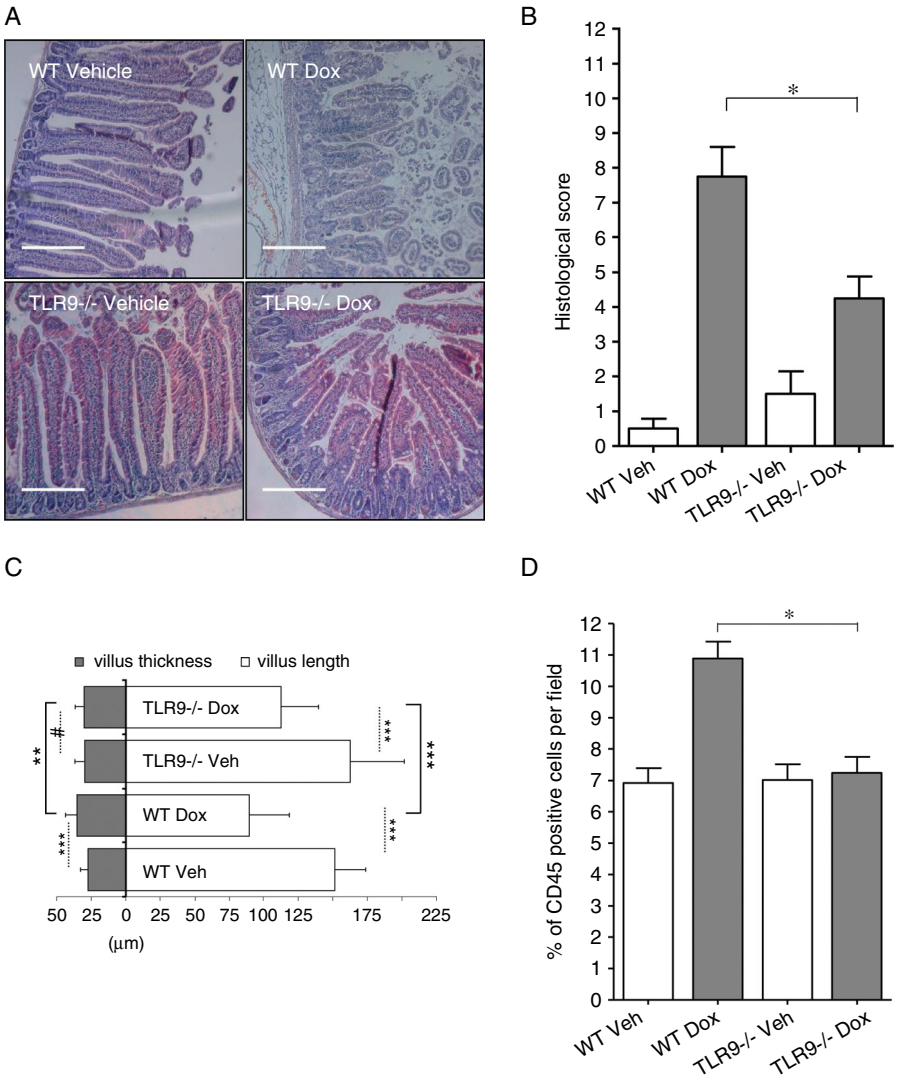

Figure 3. TLR-$9^{-/-}$ mice develop less severe mucositis after doxorubicin administration. (A) Representative images of H&E-stained sections of the ileum of WT and TLR-$9^{-/-}$ mice 72 h after doxorubicin or vehicle administration. Scale bars = 200 μm. (B) Ileum of TLR-$9^{-/-}$ and WT mice was examined and given a histological score (HS) 72 h after doxorubicin administration. The lower HS in TLR-$9^{-/-}$-deficient mice indicates better preservation of the structure of the ileum. (C) Changes in villus length (white bars) and thickness (grey bars). Villi of TLR-$9^{-/-}$ mice after doxorubicin treatment were significantly longer than villi of WT mice and their thickness was unchanged. (D) Infiltration of $CD45^{+}$ leukocytes into the lamina propria after doxorubicin administration was reduced in TLR-$9^{-/-}$ mice. $n = 4$ mice per group. $^{***}p < 0.001$; $^{**}p < 0.01$; $^{*}p < 0.05$; # non-significant difference.

become shorter or thicker, while important changes were observed in WT villi (Figure 3C). The percentage of $CD45^+$ leukocytes was smaller in TLR-$9^{-/-}$ mice (7.23% ± 1.93%) than in WT mice (10.89% ± 1.96% in WT) (Figure 3D).

Lack of TLR-2 or TLR-9 signalling increases the survival of enterocytes after doxorubicin treatment

Having demonstrated that most apoptotic events occur within 24 h after doxorubicin treatment (Figure 1D), we investigated whether the absence of TLR-2 or TLR-9 signalling can influence the survival of cells and thus contribute to the decreased histological signs of intestinal mucositis. TUNEL assay of ileum tissue sections revealed significantly fewer apoptotic cells in crypts of TLR-2- (1.26 ± 0.95) and TLR-9-deficient mice (0.68 ± 0.45) compared with WT mice (2.26 ± 0.88) (Figures 4A and 4B).

TLR-9 antagonist mitigates the severity of doxorubicin-induced intestinal mucositis

Because deficiency of TLR-2 or TLR-9 reduced the signs of doxorubicin-induced intestinal mucositis, we hypothesized that treatment of WT animals with TLR antagonists could protect them against this side effect of doxorubicin. Several TLR antagonists are commercially available, but we are unaware of any TLR-2 antagonists. We therefore tested our hypothesis by blocking TLR-9 signalling using ODN2088 [33]. WT animals were injected with doxorubicin alone or with doxorubicin combined with ODN2088. Co-administration of ODN2088 provided significant protection of intestinal villi against doxorubicin. Neither villus blunting nor atrophy was observed (Figure 5A). By contrast, mice treated only with doxorubicin showed all the signs of severe intestinal damage. HS was decreased, by an average of 43% after ODN treatment (Figure 5B). Villus shape and thickness in the ileum remained unchanged (Figure 5C) and the percentage of $CD45^+$ leukocytes dropped to control level in ODN-treated animals but was significantly elevated in mice treated only with doxorubicin (Figure 5D).

Absence of TLR-2 decreases the severity of doxorubicin-induced intestinal mucositis by increasing inhibitory phosphorylation of GSK-3β

GSK-3β is a ubiquitously expressed multifunctional kinase that influences a variety of cellular processes [34]. Several reports have shown that GSK-3β facilitates the functioning of the intrinsic apoptotic pathway

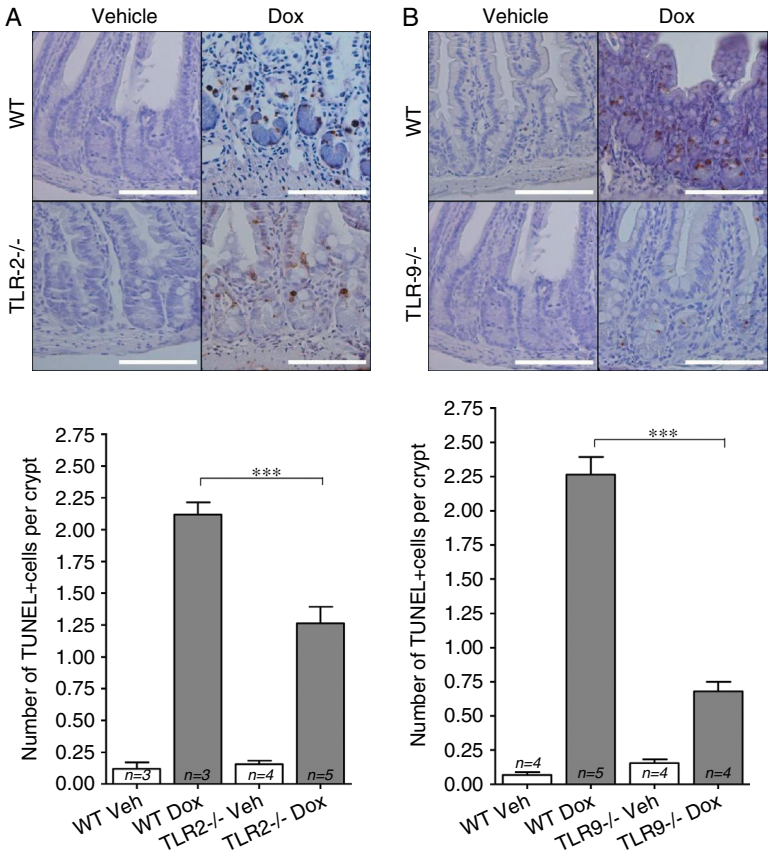

Figure 4. TLR-2 and TLR-9 are required for doxorubicin-induced apoptosis in intestinal crypts. Ileum of WT, TLR-$2^{-/-}$, and TLR-$9^{-/-}$ mice was collected 24 h after doxorubicin administration and sections were stained using TUNEL to visualize apoptotic cells. The number of apoptotic cells per crypt was significantly lower in TLR-$2^{-/-}$ (A) and TLR-$9^{-/-}$ (B) mice; *n* represents the number of mice. Insets: representative images of TUNEL-stained sections 24 h after vehicle or doxorubicin injection in TLR-$2^{-/-}$ (A) and TLR-$9^{-/-}$ mice (B). Scale bars = 100 μm. $^{***}p < 0.001$; # non-significant difference.

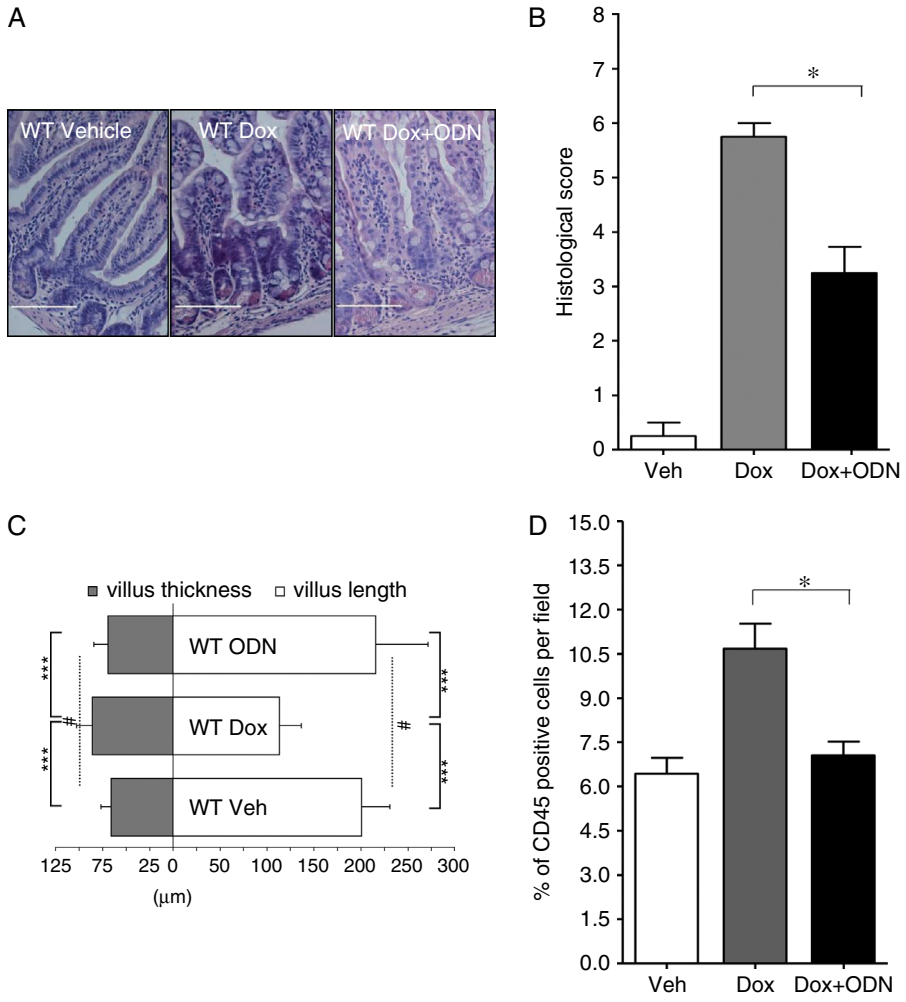

Figure 5. Administration of a TLR-9 antagonist decreases the severity of doxorubicin-induced mucositis. WT mice were treated with doxorubicin only or with doxorubicin and a TLR-9 antagonist (ODN2088). Intestinal samples were collected 72 h after treatment. (A) H&E-stained sections revealed reduced signs of intestinal damage in mice treated with ODN2088. Scale bars = 100 μm. (B) Mice receiving combined therapy developed less severe mucositis (lower HS) than mice treated with doxorubicin alone. (C) Measurement of villus length (white bars) and thickness (grey bars) showed that the TLR-9 antagonist protected ileum villi from shortening and blunting. (D) Inhibition of TLR-9 signalling by ODN2088 caused a decrease in the percentage of $CD45^+$ cells. $n = 4$ mice per group. $^{***}p < 0.001$; $^{*}p < 0.05$; # non-significant difference.

initiated by DNA-damaging drugs and by oxidative or ER stress [21]. We observed that doxorubicin injection in WT mice induced time-dependant phosphorylation of GSK-3β at Ser9, which inhibits its activity (Figure 6A). Decreased GSK-3β activity coincided with the decrease in the number of TUNEL-positive cells at later time points (48 and 72 h, Figure 1D). This prompted us to analyse whether the phosphorylation status of GSK-3β might contribute to the protection of TLR-2- and TLR-9-deficient mice against intestinal mucositis. Inhibitory phosphorylation of GSK-3β was increased at 24 h after injection in TLR-$2^{-/-}$ mice (Figure 6B), which might explain the decreased number of apoptotic cells. Interestingly, we observed only basal levels of inhibitory phosphorylation in TLR-9-deficient mice (data not shown), indicating that probably different mechanisms contribute to reducing the number of apoptotic cells and to protection of the intestinal architecture.

Inhibition of GSK-3β protects WT mice from doxorubicin-induced intestinal mucositis

The observation that GSK-3β inhibition was accompanied by a pro-survival effect in the absence of TLR-2 led us to investigate whether we could decrease apoptosis and protect the intestine against doxorubicin by using the GSK-3β inhibitor SB216763 in WT mice. Indeed, combining SB216763 with doxorubicin treatment protected the small intestine from the cytotoxicity (Figure 7A). The HS of mice pretreated with the inhibitor before doxorubicin injection was on average 1.6 times lower than the HS of mice treated with doxorubicin only (Figure 7B). Moreover, this combined therapy resulted in a 1.5-fold decrease in the number of apoptotic cells observed 24 h after doxorubicin administration (Figure 7C). This decrease in apoptosis was accompanied by increased inhibitory phosphorylation of GSK-3β after 24 h (Figure 7D).

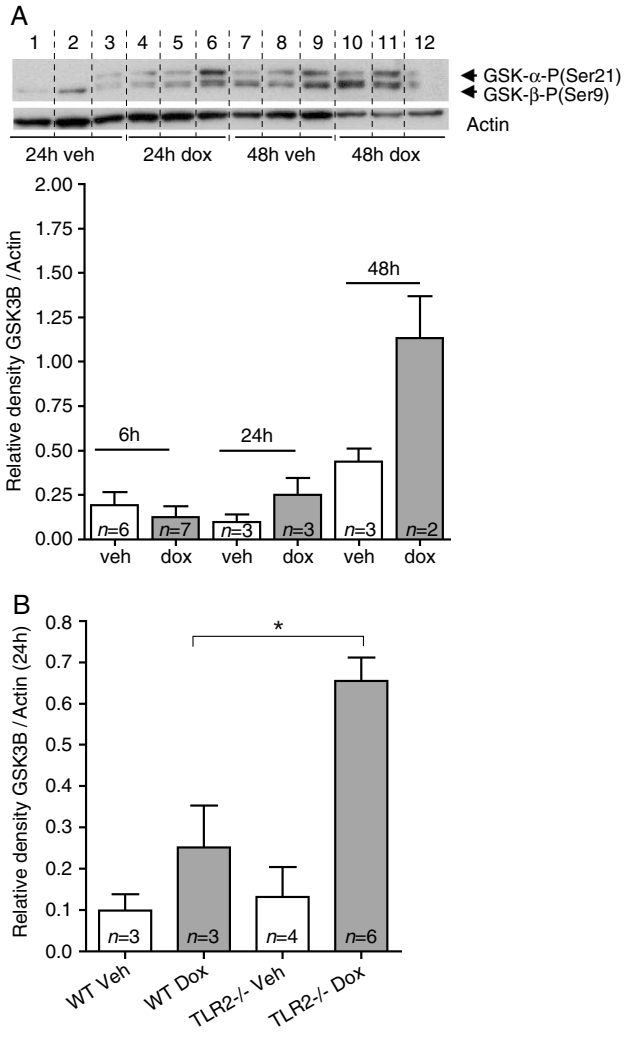

Figure 6. Inhibitory phosphorylation of GSK-3β is increased in TLR-$2^{-/-}$ mice after doxorubicin administration. Lysates of intestine were blotted for inhibitory phosphorylation (Ser9) of GSK-3β. Results are expressed as the density of the GSK-3β band relative to the actin band. (A) Representative western blot of GSK-3 phosphorylation in time kinetics and its quantification. Lanes 1–3 and 7–9: mice injected with vehicle. Lanes 4–6, and 10–12: mice injected with doxorubicin. Time indicates the time of intestine collection. Inhibitory phosphorylation of GSK-3β in WT mice increased with time after doxorubicin administration. (B) Twenty-four hours after doxorubicin injection, TLR-$2^{-/-}$ mice showed significantly more inhibition of GSK-3β than WT mice. Inhibitory phosphorylation of GSK-3β was increased as early as 24 h after injection in TLR-$2^{-/-}$ mice. *n* represents the number of mice. $^{*}p < 0.05$.

Discussion

Mucositis is a serious complication in patients undergoing anti-cancer treatment and frequently limits the use of radiation and chemotherapy [2]. Therefore, there is a compelling need for a better understanding of the endogenous mechanisms of mucositis development. In the present study, we used a mouse model of doxorubicin-induced intestinal mucositis to show for the first time that TLR-2 or TLR-9 deficiency significantly ameliorates the signs of ileitis caused by drug administration.

A harmful role of TLRs has been shown in other models of intestinal damage. For example, it has been shown in the model of Graft-versus-host disease (GvHD), a major GIT complication after allogeneic bone marrow transplantation, that TLR9$^{-/-}$ mice had reduced intestinal damage and increased survival [35,36]. Also, it has been proposed that stimulation of TLR-3 by double-stranded DNA contributes to the severity of intestinal damage [37]. However, TLR signalling under certain conditions might be protective. It has been shown that mice deficient in TLR-2 or TLR-9 are more susceptible to DSS-induced colitis [38,39]. Additionally, flagellin administration (TLR-5 stimulation) protected the gut from ionizing radiation [40–42]. The discrepancies between these studies might be explained by the different models used and the organs studied (DSS-induced colitis versus doxorubicin-induced ileitis) and by the diversity of TLR expression along the GIT [14,43]. On the other hand, these contradictory studies strongly suggest that activation of TLRs could be a double-edged sword that can be either beneficial or detrimental to intestinal integrity.

A possible explanation for the amelioration of MBI severity in our model is that absence of TLR-2 or TLR-9 decreases doxorubicin-induced apoptosis in intestinal crypts (Figures 5A and 5B). It has also been observed that TLR stimulation can lead to caspase-dependent apoptosis [44,45] and several recent studies demonstrated a crucial role for TLRs in apoptosis in a variety of cells. For example, TLR-2 is required for opioid-induced neuronal apoptosis [25], and TLR-9 deficiency results in resistance to *M. tuberculosis*-induced apoptosis *in vivo* [23] and prevents morphine-induced microglia apoptosis [24]. Therefore, in contrast to the model proposed by Sonis [4,5], our findings suggest a role for TLRs in protecting epithelial cells from the apoptosis induced by cytotoxic therapy before bacterial translocation and intestinal ulceration occur.

GSK-3 is a ubiquitous serine/threonine kinase known as an important molecular switch between apoptosis and cell survival [21]. This constitutively active kinase is regulated by phosphatidylinositol 3-kinase (PI3-K)/Akt signalling, which is also downstream of the TLR pathway [46–48]. Here, we investigated the status of inhibitory phosphorylation of GSK-3β in WT and TLR-2 or TLR-9 knockout mice in doxorubicin-induced intestinal mucositis. Inhibitory phosphorylation of GSK-3β in WT mice increased 48 and 72 h after doxorubicin injection (Figures 6A and 6B). This rather late increase in inhibitory phosphorylation probably reflects pro-survival signalling, as indicated by the reduction of apoptosis at these late time points (Figure 1D). GSK-3β inhibitory phosphorylation was up-regulated in TLR-2-deficient mice, which could explain the low levels of apoptosis in the intestinal crypts. In our model of mucositis, inhibition of GSK-3β reduced the rate of apoptosis and the severity of intestinal damage (Figures 6A and 6B), which is in agreement with a previous observation that GSK-3

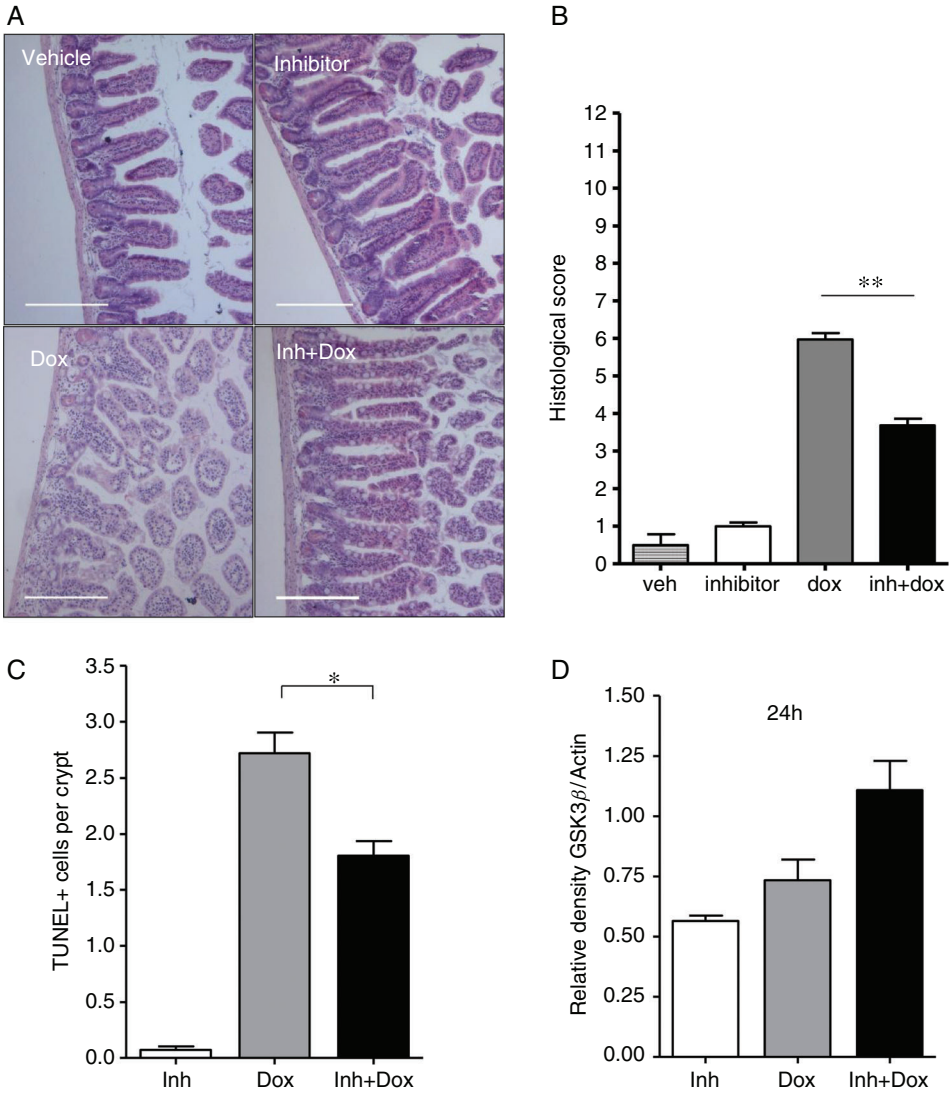

Figure 7. Pharmaceutical inhibition of GSK-3β contributes to protection against doxorubicin-induced intestinal mucositis in WT mice. WT mice were pretreated with GSK-3 inhibitor (SB216763) for two consecutive days before doxorubicin administration. (A) Representative images of H&E-stained sections of the ileum of WT mice 72 h after doxorubicin injection and HS (B). Scale bars = 100 μm. (C) Inhibition of GSK-3 influences the number of TUNEL-positive cells in WT mice. (D) Increased inactivation of GSK-3β after SB216763 treatment 24 h after doxorubicin administration. $n = 4$ mice per group. $^{**}p < 0.01$; $^{*}p < 0.05$.

inhibition protected the small intestine from radiation-induced IBM [30]. However, modulation of the cell death or survival decision by GSK-3β is complex, and the decision to switch on apoptotic or survival mechanisms could be different in other model systems [21].

Considering that TLRs are components of the first line of immune responses, there is considerable interest in the therapeutic targeting of these receptors by using either TLR agonists or antagonists, depending on the clinical application [49]. We propose that a TLR-9 antagonistic ODN can have a therapeutic effect on doxorubicin-induced intestinal mucositis. Our data are in line with the use of ODNs in the experimental treatment of IBD [50,51] and GvHD [36]. It has been shown that oral or intraperitoneal administration of inhibitory adenoviral ODN decreases inflammation in DSS-induced colitis and in a model of severe combined immunodeficiency colitis [50,51]. Together, these data point to a possible therapeutic strategy to reduce the severity of intestinal mucositis by using TLR-9 antagonists. However, additional studies will have to be performed to address the safety of this antagonist and to evaluate its effect on the efficacy of anti-cancer treatment.

Acknowledgment

We thank Dr A Cauwels (for TLR-$2^{-/-}$ mice) and Professor S Magez (for TLR-$9^{-/-}$ mice). This work was supported by a project grant from the Fund for Scientific Research Flanders (FWO-Vlaanderen, G.0728.10 to DVK) and by an individual research grant from FWO-Vlaanderen (31507110 to DVK). DVK is a post-doctoral fellow and AK is a doctoral fellow, both paid by fellowships from FWO-Vlaanderen. Vandenabeele's group is supported by VIB, Ghent University (GROUP-ID Consortium of the UGent MRP initiative), FWO-Vlaanderen (G.0875.11 and G.0973.11), Federal

Research Programme (IAP 6/18), European Research Programme FP6 ApopTrain (MRTN-CT-035624), FP7 Apo-Sys 200767, and the Euregional PACTII. PV holds a Methusalem grant (BOF09/01M00709) from the Flemish Government. We thank Dr A Bredan for editing the manuscript.

Author contribution statement

AK contributed substantially to the study design, acquisition of most of the data as well as analysis/interpretation of data, and played a major role in drafting of the manuscript. BMK contributed towards some of the data acquisition, data analysis, and critical revising of the manuscript. LH contributed towards data acquisition. PV contributed towards study design, data analysis, and interpretation. DVK played a substantially major role in conception as well as in design of the study, data acquisition, analysis and interpretation, and drafting as well as critical revising of the manuscript.

References

1. Blijlevens NM, Donnelly JP, De Pauw BE. Mucosal barrier injury: biology, pathology, clinical counterparts and consequences of intensive treatment for haematological malignancy: an overview. *Bone Marrow Transplant* 2000; **25**: 1269–1278.
2. Elting LS, Cooksley C, Chambers M, *et al*. The burdens of cancer therapy. Clinical and economic outcomes of chemotherapy-induced mucositis. *Cancer* 2003; **98**: 1531–1539.
3. van der Velden WJ, Herbers AH, Feuth T, *et al*. Intestinal damage determines the inflammatory response and early complications in patients receiving conditioning for a stem cell transplantation. *PLoS One* 2010; **5**: e15156.
4. Sonis ST. The pathobiology of mucositis. *Nature Rev Cancer* 2004; **4**: 277–284.
5. Sonis ST. New thoughts on the initiation of mucositis. *Oral Dis* 2010; **16**: 597–600.
6. Logan RM, Gibson RJ, Bowen JM, *et al*. Characterisation of mucosal changes in the alimentary tract following administration of irinotecan: implications for the pathobiology of mucositis. *Cancer Chemother Pharmacol* 2008; **62**: 33–41.
7. Logan RM, Stringer AM, Bowen JM, *et al*. Is the pathobiology of chemotherapy-induced alimentary tract mucositis influenced by the type of mucotoxic drug administered? *Cancer Chemother Pharmacol* 2009; **63**: 239–251.
8. Blijlevens NM, Lutgens LC, Schattenberg AV, *et al*. Citrulline: a potentially simple quantitative marker of intestinal epithelial damage following myeloablative therapy. *Bone Marrow Transplant* 2004; **34**: 193–196.
9. Lutgens LC, Blijlevens NM, Deutz NE, *et al*. Monitoring myeloablative therapy-induced small bowel toxicity by serum citrulline concentration: a comparison with sugar permeability tests. *Cancer* 2005; **103**: 191–199.
10. Cario E, Rosenberg IM, Brandwein SL, *et al*. Lipopolysaccharide activates distinct signaling pathways in intestinal epithelial cell lines expressing Toll-like receptors. *J Immunol* 2000; **164**: 966–972.
11. Vaishnava S, Behrendt CL, Ismail AS, *et al*. Paneth cells directly sense gut commensals and maintain homeostasis at the intestinal host–microbial interface. *Proc Natl Acad Sci U S A* 2008; **105**: 20858–20863.
12. Podolsky DK, Gerken G, Eyking A, *et al*. Colitis-associated variant of TLR2 causes impaired mucosal repair because of TFF3 deficiency. *Gastroenterology* 2009; **137**: 209–220.
13. Bogunovic M, Dave SH, Tilstra JS, *et al*. Enteroendocrine cells express functional Toll-like receptors. *Am J Physiol Gastrointest Liver Physiol* 2007; **292**: G1770–G1783.
14. Chabot S, Wagner JS, Farrant S, *et al*. TLRs regulate the gatekeeping functions of the intestinal follicle-associated epithelium. *J Immunol* 2006; **176**: 4275–4283.
15. Rakoff-Nahoum S, Paglino J, Eslami-Varzaneh F, *et al*. Recognition of commensal microflora by toll-like receptors is required for intestinal homeostasis. *Cell* 2004; **118**: 229–241.
16. Vora P, Youdim A, Thomas LS, *et al*. Beta-defensin-2 expression is regulated by TLR signaling in intestinal epithelial cells. *J Immunol* 2004; **173**: 5398–5405.
17. Kawai T, Akira S. The role of pattern-recognition receptors in innate immunity: update on Toll-like receptors. *Nature Immunol* 2010; **11**: 373–384.
18. Fukata M, Vamadevan AS, Abreu MT. Toll-like receptors (TLRs) and Nod-like receptors (NLRs) in inflammatory disorders. *Semin Immunol* 2009; **21**: 242–253.
19. Beurel E, Michalek SM, Jope RS. Innate and adaptive immune responses regulated by glycogen synthase kinase-3 (GSK3). *Trends Immunol* 2010; **31**: 24–31.
20. Martin M, Rehani K, Jope RS, *et al*. Toll-like receptor-mediated cytokine production is differentially regulated by glycogen synthase kinase 3. *Nature Immunol* 2005; **6**: 777–784.
21. Beurel E, Jope RS. The paradoxical pro- and anti-apoptotic actions of GSK3 in the intrinsic and extrinsic apoptosis signaling pathways. *Prog Neurobiol* 2006; **79**: 173–189.
22. Hofmann C, Dunger N, Scholmerich J, *et al*. Glycogen synthase kinase 3-beta: a master regulator of toll-like receptor-mediated chronic intestinal inflammation. *Inflamm Bowel Dis* 2010; **16**: 1850–1858.
23. Chen L, Shi W, Li H, *et al*. Critical role of toll-like receptor 9 in morphine and *Mycobacterium tuberculosis*-induced apoptosis in mice. *PLoS One* 2010; **5**: e9205.
24. He L, Li H, Chen L, *et al*. Toll-like receptor 9 is required for opioid-induced microglia apoptosis. *PLoS One* 2011; **6**: e18190.
25. Li Y, Li H, Zhang Y, *et al*. Toll-like receptor 2 is required for opioids-induced neuronal apoptosis. *Biochem Biophys Res Commun* 2011; **391**: 426–430.
26. Keefe DM, Brealey J, Goland GJ, *et al*. Chemotherapy for cancer causes apoptosis that precedes hypoplasia in crypts of the small intestine in humans. *Gut* 2000; **47**: 632–637.
27. de Koning BA, van Dieren JM, Lindenbergh-Kortleve DJ, *et al*. Contributions of mucosal immune cells to methotrexate-induced mucositis. *Int Immunol* 2006; **18**: 941–949.
28. Imaeda AB, Watanabe A, Sohail MA, *et al*. Acetaminophen-induced hepatotoxicity in mice is dependent on Tlr9 and the Nalp3 inflammasome. *J Clin Invest* 2009; **119**: 305–314.
29. Coghlan MP, Culbert AA, Cross DA, *et al*. Selective small molecule inhibitors of glycogen synthase kinase-3 modulate glycogen metabolism and gene transcription. *Chem Biol* 2000; **7**: 793–803.
30. Thotala DK, Geng L, Dickey AK, *et al*. A new class of molecular targeted radioprotectors: GSK-3beta inhibitors. *Int J Radiat Oncol Biol Phys* 2010; **76**: 557–565.
31. Krysko DV, Vanden Berghe T, Parthoens E, *et al*. Methods for distinguishing apoptotic from necrotic cells and measuring their clearance. *Methods Enzymol* 2008; **442**: 307–341.

32. Krysko DV, Kaczmarek A, Krysko O, *et al*. TLR-2 and TLR-9 are sensors of apoptosis in a mouse model of doxorubicin-induced acute inflammation. *Cell Death Differ* 2011; **18**: 1316–1325.
33. Duramad O, Fearon KL, Chang B, *et al*. Inhibitors of TLR-9 act on multiple cell subsets in mouse and man *in vitro* and prevent death *in vivo* from systemic inflammation. *J Immunol* 2005; **174**: 5193–5200.
34. Cohen P, Frame S. The renaissance of GSK3. *Nature Rev Mol Cell Biol* 2001; **2**: 769–776.
35. Calcaterra C, Sfondrini L, Rossini A, *et al*. Critical role of TLR9 in acute graft-versus-host disease. *J Immunol* 2008; **181**: 6132–6139.
36. Heimesaat MM, Nogai A, Bereswill S, *et al*. MyD88/TLR9 mediated immunopathology and gut microbiota dynamics in a novel murine model of intestinal graft-versus-host disease. *Gut* 2010; **59**: 1079–1087.
37. Zhou R, Wei H, Sun R, *et al*. Recognition of double-stranded RNA by TLR3 induces severe small intestinal injury in mice. *J Immunol* 2007; **178**: 4548–4556.
38. Cario E, Gerken G, Podolsky DK. Toll-like receptor 2 controls mucosal inflammation by regulating epithelial barrier function. *Gastroenterology* 2007; **132**: 1359–1374.
39. Lee J, Mo JH, Katakura K, *et al*. Maintenance of colonic homeostasis by distinctive apical TLR9 signalling in intestinal epithelial cells. *Nature Cell Biol* 2006; **8**: 1327–1336.
40. Jones RM, Sloane VM, Wu H, *et al*. Flagellin administration protects gut mucosal tissue from irradiation-induced apoptosis via MKP-7 activity. *Gut* 2011; **60**: 648–657.
41. Vijay-Kumar M, Aitken JD, Sanders CJ, *et al*. Flagellin treatment protects against chemicals, bacteria, viruses, and radiation. *J Immunol* 2008; **180**: 8280–8285.
42. Burdelya LG, Krivokrysenko VI, Tallant TC, *et al*. An agonist of toll-like receptor 5 has radioprotective activity in mouse and primate models. *Science* 2008; **320**: 226–230.
43. Abreu MT. Toll-like receptor signalling in the intestinal epithelium: how bacterial recognition shapes intestinal function. *Nature Rev Immunol* 2010; **10**: 131–144.
44. Into T, Kiura K, Yasuda M, *et al*. Stimulation of human Toll-like receptor (TLR) 2 and TLR6 with membrane lipoproteins of *Mycoplasma fermentans* induces apoptotic cell death after NF-kappa B activation. *Cell Microbiol* 2004; **6**: 187–199.
45. Jung DY, Lee H, Jung BY, *et al*. TLR4, but not TLR2, signals autoregulatory apoptosis of cultured microglia: a critical role of IFN-beta as a decision maker. *J Immunol* 2005; **174**: 6467–6476.
46. Jope RS, Johnson GV. The glamour and gloom of glycogen synthase kinase-3. *Trends Biochem Sci* 2004; **29**: 95–102.
47. Akira S, Takeda K. Toll-like receptor signalling. *Nature Rev Immunol* 2004; **4**: 499–511.
48. Woodgett JR, Ohashi PS. GSK3: an in-Toll-erant protein kinase? *Nature Immunol* 2005; **6**: 751–752.
49. Kanzler H, Barrat FJ, Hessel EM, *et al*. Therapeutic targeting of innate immunity with Toll-like receptor agonists and antagonists. *Nature Med* 2007; **13**: 552–559.
50. Obermeier F, Strauch UG, Dunger N, *et al*. *In vivo* CpG DNA/toll-like receptor 9 interaction induces regulatory properties in CD4+CD62L+ T cells which prevent intestinal inflammation in the SCID transfer model of colitis. *Gut* 2005; **54**: 1428–1436.
51. Obermeier F, Dunger N, Strauch UG, *et al*. CpG motifs of bacterial DNA essentially contribute to the perpetuation of chronic intestinal inflammation. *Gastroenterology* 2005; **129**: 913–927.

SUPPORTING INFORMATION ON THE INTERNET

The following supporting information may be found in the online version of this article.

Table S1. Criteria used to assess damage of doxorubicin-induced intestinal mucositis.